Formation of a coplanar O–Al bonding cluster: the effect of O impurity on a Σ = 5 NiAl grain boundary from first-principles

2009 J. Phys.: Condens. Matter 21 015002

(http://iopscience.iop.org/0953-8984/21/1/015002)

J. Phys.: Condens. Matter **21** (2009) 015002 (7pp) doi:10.1088/0953-8984/21/1/015002

Formation of a coplanar O–Al bonding cluster: the effect of O impurity on a $\Sigma = 5$ NiAl grain boundary from first-principles

Li-Hua Liu, Ying Zhang, Xue-Lan Hu and Guang-Hong Lu[1]

Department of Physics, Beijing University of Aeronautics and Astronautics, Beijing 100191, People's Republic of China

Received 1 September 2008, in final form 24 October 2008
Published 1 December 2008
Online at stacks.iop.org/JPhysCM/21/015002

Abstract

The site occupancy, structure, and bonding properties of O in an NiAl grain boundary (GB) have been investigated by employing a first-principles total energy method based on density functional theory with the generalized gradient approximation and ultrasoft pseudopotential. The $\Sigma5(310)/[001]$ tilt GB of NiAl has been chosen because (i) the $\Sigma = 5$ GB has been observed to be a higher fraction in NiAl experimentally, and (ii) the $\Sigma5(310)/[001]$ is energetically favorable in comparison with the $\Sigma5(210)/[001]$. The NiAl GB is shown to favor the O segregation with a segregation energy of -1.75 eV, indicating that most of the O impurity will distribute in the NiAl GB thermodynamically. Moreover, O is shown to prefer occupying the interstitial sites rather than the substitutional sites in the GB according to the calculated formation energies. The O–Al bond is energetically favorable as compared with the O–Ni bond due to different electronegativity of Al and Ni in reference to O. Charge distribution and the density of states further indicate the intrinsic bonding properties of O–Al that contain obvious covalent characteristics. It is interesting to find that O is coplanar with the surrounding Al atoms in both interstitial and substitutional cases with lower formation energies, forming stronger coplanar O–Al bonding clusters. Such stronger bonding clusters in the GB can embrittle the NiAl intermetallics and thus are not beneficial to the plasticity of NiAl. Our results will provide a useful reference for improving the mechanical properties and for understanding the oxidation effect of the NiAl intermetallics.

(Some figures in this article are in colour only in the electronic version)

1. Introduction

Nickel aluminum (NiAl) intermetallics exhibit many good properties including high strength, high melting temperature, and good corrosion resistance, and thus can be applied in the aerospace industry as high temperature structural materials [1, 2]. However, poor ductility at low temperatures and low strength at elevated temperature limits their applications. Many efforts have been made to focus primarily on improving the mechanical properties of NiAl mainly by adding alloying elements such as Cr, Mo, Hf, and Dy [3–5].

Several kinds of impurities can exist in the NiAl including O, B, C, N, Si, P, and S [1]. Most of these impurities are considered to be deleterious to the mechanical properties of NiAl, and they generally segregate in grain boundaries (GBs). Segregation of a trace amount (ppm) of impurity in the GB can greatly change the GB structure, resulting in a large variation of the mechanical properties of materials [6–11]. Experimental observations show that NiAl is brittle at room temperature and normally breaks intergranularly [7, 12], indicating the crucial role of GBs in determining the mechanical properties of NiAl. The GBs have thus been an important subject of many studies over the past few decades [5–13].

[1] Author to whom any correspondence should be addressed.

It is reported that impurity elements such as B and P can easily segregate in the GBs [1, 7, 12]. B can even change the fracture mode of NiAl from intergranular to transgranular cleavage despite the ductility not being improved [7, 12]. The role of segregation of alloying elements such as Nd [14] and Zr [15] on the NiAl GBs has also been investigated experimentally. In addition, the $\Sigma = 5$ GB has been shown to be strong and to have a good crack resistance, leading to its higher fraction in NiAl [16]. Theoretically, an empirical potential has been constructed for NiAl, which can reproduce the asymmetric properties of constitutional point defects [17]. Such potential has been applied to NiAl GBs, demonstrating different segregation behaviors of Ni and Al in the NiAl GBs [17]. Significant Ni segregation is found at the NiAl GBs, leading to boundary transformations to new structures capable of accommodating more excess Ni atoms as compared with the initial structure [18, 19]. Further, the $\Sigma5(310)$ GB has been shown to be more stable than the $\Sigma5(210)$ one according to the simulated GB energies [20]. Moreover, the effect of B on an FeAl $\Sigma5(310)$ GB with the same B2 structure as NiAl has also been investigated by the first-principles method [21].

A small amount of impurity such as O is being considered to have large effects on the structure and mechanical properties of NiAl. So far, however, only very few studies have been devoted to understanding the effects of O in NiAl. We have already investigated the effects of O on the structure and mechanical properties of the *bulk* NiAl using a first-principles method [22], and found that O tends to form an Al_2O_3-like tetrahedron structure with its nearest Al or Ni atoms, leading to the formation of the stronger O–Al bond containing covalent component. This can cause an increase of the brittleness and a decrease of the ductility of NiAl based on the calculated elastic constants and the empirical criteria. In this paper, we perform a first-principles calculation to investigate the atomic and electronic structures of NiAl GB with the O impurity. The purpose of this paper is to explore and understand the effects of O on the NiAl GB. A significant part of this paper has been directed towards finding the stable site for O in the NiAl GBs and understanding the bonding mechanism of O based on the calculated formation and segregation energies. Our calculations will provide a reference for improving the mechanical properties of the NiAl intermetallics and can also be helpful in understanding its oxidation effect.

2. Computational method

We employ a first-principles total energy method based on density functional theory with generalized gradient approximation according to the parametrization of Perdew and Wang [23] and ultrasoft pseudopotential as implemented in VASP [24, 25]. The plane-wave energy cutoff is 340 eV. The energy relaxation iterates until the forces on all the atoms are less than 10^{-3} eV Å^{-1}. We deal with an NiAl $\Sigma = 5(310)/[001]$ tilt grain boundary, which is a typical coincidence boundary in NiAl. It is formed by rotating a grain by 36.9° along the [001] axis and (310) is set as the boundary plane. The supercell is constructed as shown in figure 1. The length in the [001] direction is set to be twice that of the CSL, in order to retain the symmetry of the configuration. In the [310] direction, two symmetric boundaries are introduced to make the three-dimensional periodicity. The supercell size is $19.38 \times 9.10 \times 5.65$ Å^3, sampled by a $(2 \times 4 \times 8)$ special k-point grid according to the Monkhorst–Pack scheme [26].

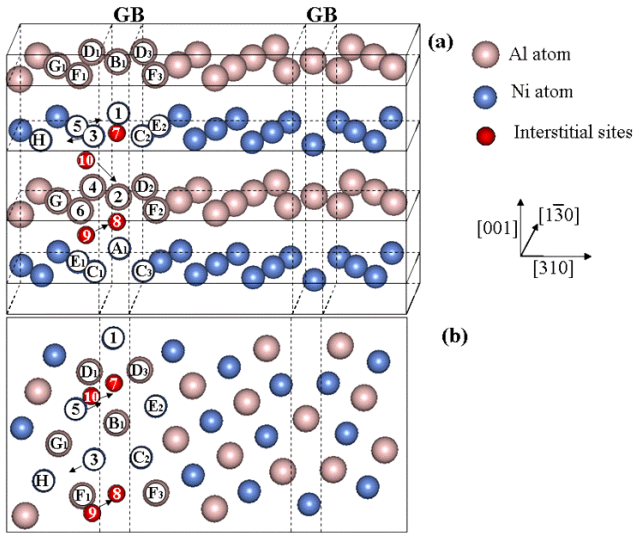

Figure 1. (a) The supercell of $\Sigma5(310)/[001]$ title NiAl GB, (b) top view of the supercell. The supercell includes four (001) atomic layers, two Ni layers and two Al layers. Schematically, the largest purple spheres represent the Al atoms, while the second largest blue spheres represent the Ni and the smallest red spheres represent the interstitial sites, respectively. The numbers 1, 3, and 5 represent the sites of the O substitution for Ni in the GB, and those of 2, 4, and 6 the sites of the O substitution for Al, while numbers 7–10 represent the four different interstitial sites. The letters with subscript numbers denote the Ni or Al atoms, which are for later discussion. The arrows show the shift direction after the atomic relaxation.

The $\Sigma5(310)/[001]$ tilt GBs of NiAl have been employed due to the following reasons. First of all, the $\Sigma = 5$ GB has been observed by experiment [16, 27, 28]. Such GBs have been shown to be strong and with a good crack resistance, which results in its higher fraction in NiAl [16]. Secondly, the $\Sigma5$ GB of NiAl consists of both $\Sigma5(310)/[001]$ and $\Sigma5(210)/[001]$. The lowest energy structure for the $\Sigma5(210)/[001]$ GB exhibits a GB cohesive energy of 0.772 J m^{-2}, while that for the $\Sigma5(310)/[001]$ GB exhibits a GB cohesive energy of 0.930 J m^{-2}. Obviously, the $\Sigma5(310)/[001]$ GB is energetically more stable than the $\Sigma5(210)/[001]$ one [20].

Formation energies are calculated as follows. When the O atom replaces an Ni or Al atom, the formation energy of $E_{\mathrm{O}}^{\mathrm{f}}$ can be obtained by

$$E_{\mathrm{O}}^{\mathrm{f}} = E_{\mathrm{NiAl-O}}^{\mathrm{T}} - E_{\mathrm{NiAl}}^{\mathrm{T}} - E_{\mathrm{O}} + \mu_{\mathrm{Ni/Al}} \tag{1}$$

where $E_{\mathrm{NiAl}}^{\mathrm{T}}$ and $E_{\mathrm{NiAl-O}}^{\mathrm{T}}$ are the total energies of the NiAl supercell without and with O, respectively, E_{O} is the energy of an isolated O atom, and $\mu_{\mathrm{Ni/Al}}$ is the chemical potential of one Ni or Al atom. When O occupies an interstitial site, the formation energy is expressed by

$$E_{\mathrm{O}}^{\mathrm{f}} = E_{\mathrm{NiAl-O}}^{\mathrm{T}} - E_{\mathrm{NiAl}}^{\mathrm{T}} - E_{\mathrm{O}}. \tag{2}$$

The negative impurity formation energy indicates that the NiAl–O system is more stable than the clean case, while the positive indicates that the clean case is more stable.

3. Results and discussion

3.1. Formation energy

In order to find the most favorable sites of O in the NiAl GB, we first calculate the formation energy of the respective case after the structure optimization. As shown in figure 1, the O atom has been set up in ten different sites in the GB, in which six are for substitutional and four for interstitial cases. These are the representative sites for O in the NiAl GB.

For the substitutional cases, the chemical potentials of Ni and Al atoms should be taken into account. The upper limits of the atomic chemical potentials of μ_{Ni} and μ_{Al} are those of the face-centered-cubic bulk crystalline phases, $\mu_{\mathrm{Ni}}^{\mathrm{bulk}}$ and $\mu_{\mathrm{Al}}^{\mathrm{bulk}}$. Because the Ni and Al atoms should equilibrate with the NiAl bulk, we have

$$\mu_{\mathrm{Ni}} + \mu_{\mathrm{Al}} = \mu_{\mathrm{NiAl}}^{\mathrm{bulk}} = \mu_{\mathrm{Ni}}^{\mathrm{bulk}} + \mu_{\mathrm{Al}}^{\mathrm{bulk}} - \Delta H, \tag{3}$$

where ΔH is the heat of formation of NiAl. Thus, the allowable ranges of the atomic chemical potentials can be given as

$$\mu_{\mathrm{Ni}}^{\mathrm{bulk}} - \Delta H \leqslant \mu_{\mathrm{Ni}} \leqslant \mu_{\mathrm{Ni}}^{\mathrm{bulk}} \tag{4}$$

and

$$\mu_{\mathrm{Al}}^{\mathrm{bulk}} - \Delta H \leqslant \mu_{\mathrm{Al}} \leqslant \mu_{\mathrm{Al}}^{\mathrm{bulk}}. \tag{5}$$

Let $\Delta\mu = \mu_{\mathrm{Ni}} - \mu_{\mathrm{Al}}$, then the relation of

$$\mu_{\mathrm{Ni}}^{\mathrm{bulk}} - \mu_{\mathrm{Al}}^{\mathrm{bulk}} - \Delta H \leqslant \Delta\mu \leqslant \mu_{\mathrm{Ni}}^{\mathrm{bulk}} - \mu_{\mathrm{Al}}^{\mathrm{bulk}} + \Delta H \tag{6}$$

can be obtained. According to the present calculations, $\mu_{\mathrm{Ni}}^{\mathrm{bulk}}$, $\mu_{\mathrm{Al}}^{\mathrm{bulk}}$, and $\mu_{\mathrm{NiAl}}^{\mathrm{bulk}}$ are -5.481 eV, -3.692 eV, and -10.487 eV, respectively. ΔH thus can be calculated as 1.314 eV according to equation (3). Consequently, the chemical potential difference $\Delta\mu = \mu_{\mathrm{Ni}} - \mu_{\mathrm{Al}}$ is negative, indicating that the chemical potential of the Ni atom is always lower than that of the Al atom. This implies that the Ni atom is easier to be drawn out of or put in the NiAl crystal than the Al atom. The formation energy of substitutional O for either Ni or Al in different sites as a function of chemical potential is shown in figure 2.

For convenience, we let S1, S3, and S5 represent the cases of one O atom replacing the Ni atom in the GB, and S2, S4, and S6 for the O replacing the Al atom, while I7–I10 represent the four different interstitial sites, respectively, as shown in figure 1. Overall, as shown in figure 2, the substitutional cases exhibit higher formation energies, while the interstitial cases exhibit lower formation energies. The formation energies of the Al substitutional cases of S2 and S6 are much higher in the whole range of the allowable chemical potential, and that of the S2 case is the highest. Another Al substitutional case (S4) has lower formation energy in comparison with S2 and S6, but its formation energy is still higher than that of the Ni substitutional case in an Al-rich environment. For the Ni substitutional cases, the formation energies are close to each other, indicating that

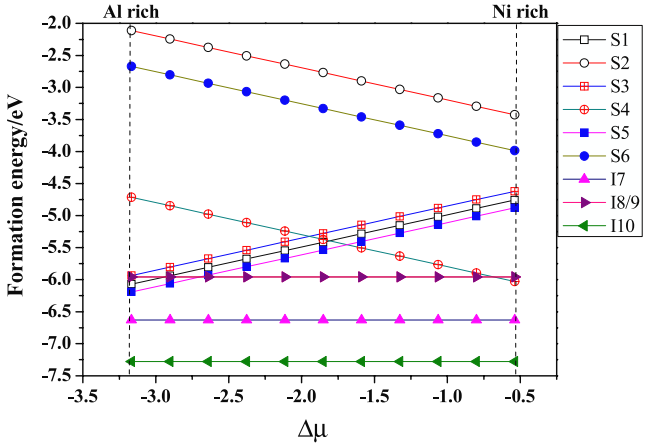

Figure 2. Formation energies of O as a function of the atomic chemical potential difference $\Delta\mu = \mu_{\mathrm{Ni}} - \mu_{\mathrm{Al}}$ between Ni and Al for the different substitutional and interstitial sites that O occupies. The lower limit of $\Delta\mu$ corresponds to $\mu_{\mathrm{Al}} = \mu_{\mathrm{Al}}^{\mathrm{bulk}}$, and the upper limit of $\Delta\mu$ corresponds to $\mu_{\mathrm{Ni}} = \mu_{\mathrm{Ni}}^{\mathrm{bulk}}$.

the effect of GB is not so large. The S4 case intersects with S1, S3, and S5 as the $\Delta\mu$ is -1.8, which indicates that O prefers replacing Ni to Al when $\Delta\mu$ is lower than -1.8, while O prefers replacing Al when $\Delta\mu$ is larger than -1.8. These results suggest that O substitution for Ni is preferable to that for Al. This is similar to the previous study [22, 29], which shows that O atoms prefer replacing Ni to Al in the NiAl bulk.

The interstitial O in GB has lower formation energy as compared with the substitutional one, which is independent of the chemical potential of the Ni or Al atoms. Thus, O prefers to occupy the interstitial sites in the NiAl GB. The formation energy for the I10 case is the lowest and the I7 case is second lowest. This is closely related to the environment in which O exists, which will be discussed in the next section.

3.2. Segregation energy

The segregation energy E_{S} of O in the NiAl GB can be calculated by

$$E_{\mathrm{S}} = \left(E_{\mathrm{GB}}^{\mathrm{O}} - E_{\mathrm{GB}}\right) - \left(E_{\mathrm{B}}^{\mathrm{O}} - E_{\mathrm{B}}\right), \tag{7}$$

where $E_{\mathrm{GB}}^{\mathrm{O}}$ and E_{GB} are the total energies of the NiAl GB system with and without O, and $E_{\mathrm{B}}^{\mathrm{O}}$ and E_{B} are the total energies of the NiAl bulk system with and without O. The NiAl bulk system crystallizes in the body-centered-cubic structure, which contains 40 Ni atoms and 40 Al atoms with nearly the same size as the corresponding GB system.

We consider the lowest formation energy case, i.e. I10. The segregation energy of O in the NiAl GB is calculated to be -1.75 eV, implying that O prefers to stay in the NiAl GBs instead of the bulk. At room temperature, we find that the O concentration in NiAl GB is much higher than in the bulk estimated by the McLean equation [9], implying that almost all the O atoms will segregate into the NiAl GBs. Furthermore, O atoms may form a thick oxidation layer when a mass of them exists in the interfaces, which is closely related to the good oxidation resistance of NiAl [1, 2].

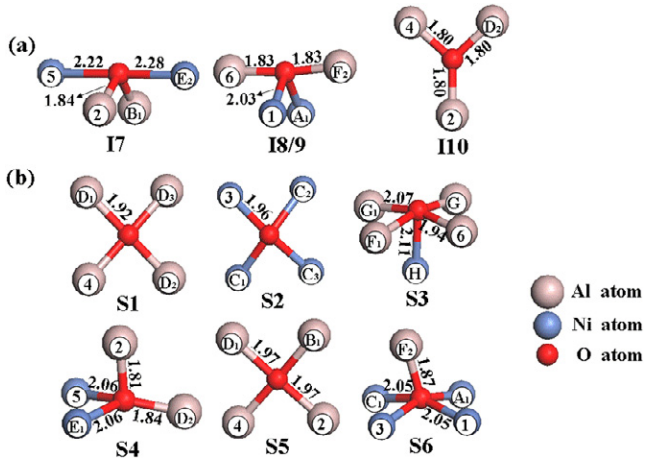

Figure 3. The atomic configuration of O and its first nearest-neighbor atoms in the NiAl GB. (a) The interstitial cases, (b) the substitutional cases. The integers and letters noted on the spheres (atoms) correspond to those noted in figure 1, while the red smallest sphere represents the O atoms, and the decimals denote the corresponding bond lengths with the unit of Å.

3.3. Atomic configuration

Now it is clear that O has a strong tendency to stay in the NiAl GBs instead of the bulk. In the GBs, the interstitial site is energetically favorable for O in comparison with the substitutional cases. Now we see how the O atom bonds with the Al and Ni atoms in the NiAl GBs according to the atomic configurations after the O segregation. For the energetically favorable interstitial cases, it is found that O will move into the center of the NiAl GBs despite it being set initially to deviate from the center of the GBs. For instance, for the I9 case, the O atom is set originally one atomic layer deviated from the GB (figure 1). Atomic relaxation makes O move to the I8 site, which is at the center of the GB. For the I10 case, O also moves into the center of the GB, and stays on one of the Al atomic layers with the lowest formation energy.

Figure 3 shows the atomic configurations of the O atom with its first nearest-neighbor (1NN) Ni or Al atoms. The interstitial cases are shown in figure 3(a). As also mentioned above, O for the I10 case moves into the Al atomic layer in the GB, surrounded by three 1NN Al atoms (4, D_2 and 2), which exhibits the lowest formation energy. The O–Al bond lengths are 1.80 Å, much shorter than that between O and its 2NN Ni atom (2.81 Å, the Ni atom denoted by 5 and E_2). Moreover, such O–Al length is similar to the O–Al length in the Al bulk case (1.77 Å) [22], but exhibits different atomic configuration with three Al atoms due to the presence of GB. In the bulk case, O tends to form an Al_2O_3-like structure with two Al atoms and two Ni atoms as its 1NN [22]. O for the I8 case almost stays at its initial site in the center of the GB, which is surrounded by two Al atoms in the Al atomic layer and two Ni atoms that are above and below the Al layer, respectively. O in the I9 site is shown to exhibit exactly the same configuration as the I8 case. Namely, O moves to the I8 site after the atomic relaxation. The bond lengths of O–Al and O–Ni are 1.83 Å and 2.03 Å, respectively. The I8/9 case is similar to the bulk case in which the bond lengths of O–Al and O–Ni are 1.77 Å and 1.99 Å, respectively [22]. The I7 case exhibits higher formation energy than the I10 case. O for this case is also surrounded by two Al and two Ni atoms. The O–Al bond length is 1.84 Å, which is larger than the I10 case. The O–Ni bond lengths are 2.22 and 2.28 Å, respectively. Both are larger than that in the I8/9 case. These results obviously show that O is preferable to bond with Al rather than Ni.

Table 1. Variation of the number of atoms and the type of the first nearest-neighbor atoms of O before and after relaxation for the different cases.

Case	Before relaxation	After relaxation
S1	8 Al	4 Al
S2	8 Ni	4 Ni
S3	1 Ni, 6 Al	4 Al, 1 Ni
S4	6 Ni, 1 Al	2 Al, 2 Ni
S5	8 Al	4 Al
S6	8 Ni	1 Al, 4 Ni
I7	2 Al, 2 Ni	2 Al, 2 Ni
I8/9	2 Al, 2 Ni	2 Al, 2 Ni
I10	2 Al, 1 Ni	3 Al

The conclusion that O favors bonding with Al can be also reflected in the substitutional cases. As mentioned above, O prefers to replace Ni in the NiAl GB, forming an Al-rich environment around O. Al replacement of O leads to a much higher formation energy, as shown for the S2 and S6 cases. The atomic configurations of the substitutional cases are shown in figure 3(b). S2 exhibits higher formation energy than S6 because all the surrounding atoms of O in the S2 case are Ni (3, C_1, C_2, and C_3) with bond length of 1.96 Å, whereas an additional Al atom (F_2) bonds with O with a bond length of 1.87 Å existing besides four Ni atoms in the S6 case. The formation energies of the remaining four substitutional cases are comparable depending on the surrounding environments. O prefers to bond with Al rather than Ni because of the larger electronegativity difference between O (3.44, Pauling) and Al (1.95) than between O and Ni (2.05) [30]. This can also be understood by the formation energies of Al_2O_3 and NiO. The formation energy of Al_2O_3 is much lower than that of NiO, showing that O energetically likes to bond with Al.

Both the interstitial and substitutional cases exhibit different configurations from the bulk case due to the presence of GB, as shown in figure 3. Variations of the number and the type of the 1NN atoms of O before and after relaxation for different cases in the NiAl GB are shown in table 1. The number of 1NN atoms is generally four atoms including either Al or Ni atoms or both, similar to the bulk case [22]. In some particular cases, the number changes to three or five due to the presence of the GB. For example, O in the I10 case bonds with only three Al atoms, while O in the S3 case bonds with one additional Ni atom as well as four Al atoms, and O in the S6 case bonds with one additional Al atom besides the four Ni atoms.

3.4. Density of states and charge distribution

The intrinsic bonding properties of the O–Al bond can be analyzed by the density of states (DOS). We chose two

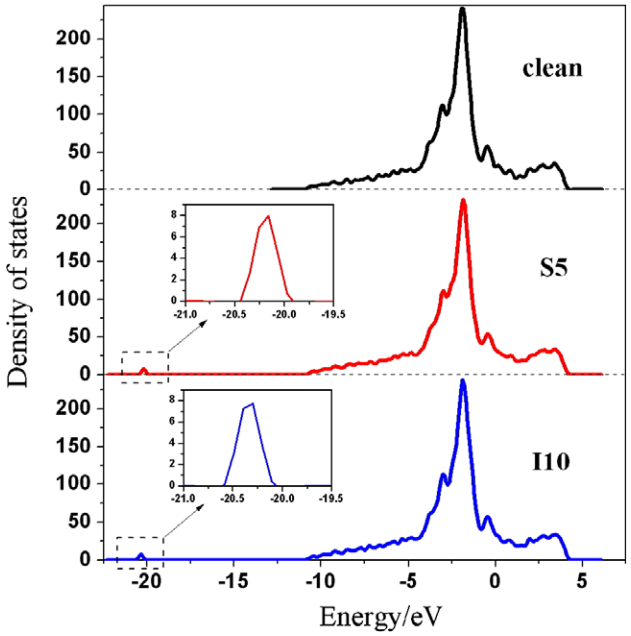

Figure 4. The total density of states for the clean, I10 and S5 cases, respectively. The Fermi energies are set as zero for all the cases.

representative lower formation energy cases, i.e. I10 and S5, among the interstitial and substitutional cases. The total DOS of these two cases are shown in figure 4. In comparison with the clean NiAl GBs, the total DOS exhibits an additional small peak in the low energy part when the O atom is introduced by replacing the Ni atoms or by directly occupying the interstitial sites in the NiAl GB. Thus, the appearance of such small peak should be straightforwardly related to the O atom. The main peaks close to the Fermi energy should correspond to the Ni–Al bonds since they remain almost unchanged after the O addition as compared with those of the clean NiAl.

In order to investigate the origin of the small peaks that appear in the total DOS due to the O introduction, we calculated the local density of states (LDOS) of O for s and p orbitals for the S5 and I10 cases with reference to that of the O gas. As shown in figure 5, O has two strong characteristic peaks, corresponding to the 2s and 2p orbitals, respectively. For the O gas, the 2p electrons mainly contribute to the O–O bonding, leading to the appearance of a much stronger peak in the higher energy part in the LDOS (the red broken line in figure 5 for the O gas case). However, when O is introduced in the NiAl GB (either substitution or interstitial), such stronger peaks in the higher energy part characterizing the 2p electrons of O become much weaker and dispersive in the LDOS of O (the red broken lines for the S5 and I10 cases). This should be closely related to the O–Al bonds since O is surrounded by the Al atoms in both cases. A similar peak to that in the LDOS in the O gas in the lower energy part appears, which is related to the 2s electrons of O, although the corresponding energies of these peaks are reduced as compared with the LDOS of the O gas. The energy values corresponding to these peaks are almost the same as those in the total DOS in figure 4 for the respective cases, suggesting that the formation of the O–Al bonds are directly related the 2s orbital of O introduced in NiAl.

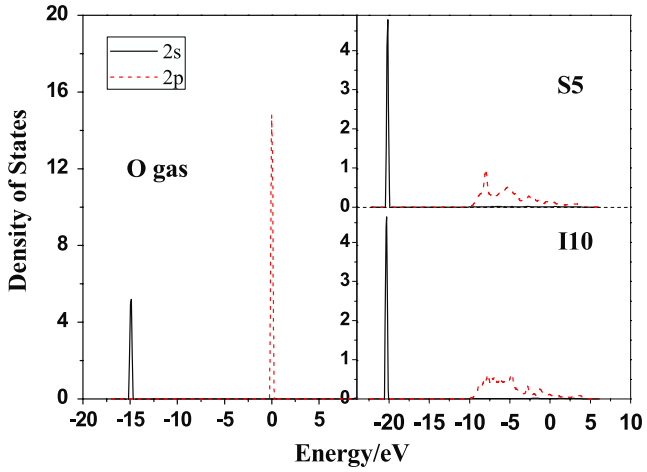

Figure 5. Local density of states for the O atom in the NiAl GB for the I10 and S5 cases as well as in the O gas. The Fermi energies are set to zero for all the cases.

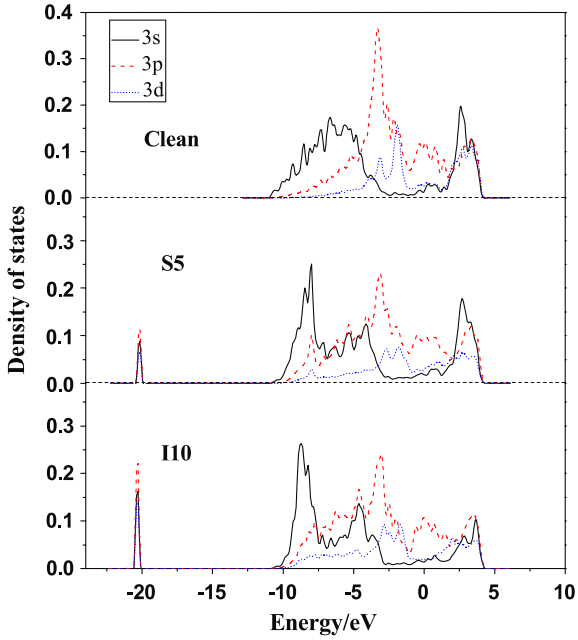

Figure 6. The local density of state of the Al atom (atom 4 noted in figure 1) as a first nearest-neighbor of O in NiAl GB for the I10 and S5 cases. The local density of state of the Al atom (the same atom 4 in figure 1) in the clean GB is also given for comparison. The Fermi energies are set as zero for all the cases.

Figure 6 gives the LDOS of Al (atom 4 noted in figure 1) with O in NiAl for the I10 and S5 cases. The LDOS of Al changes greatly as compared with that of the clean GB due to the O introduction. All the orbitals including 3s, 3p, and 3d of Al exhibit an obvious additional peak in the lower energy part, with the same energy as the O 2s peak in figure 5. This indicates a bond between O and Al forms, hybridized with the O 2s, Al 3s and 3p orbitals. In addition, in the higher energy part, the LDOS of all the orbitals of Al decreases because the number of Ni–Al bonds around Al is reduced due to the O presence. The peaks for the 3s and 3p orbital of Al in the

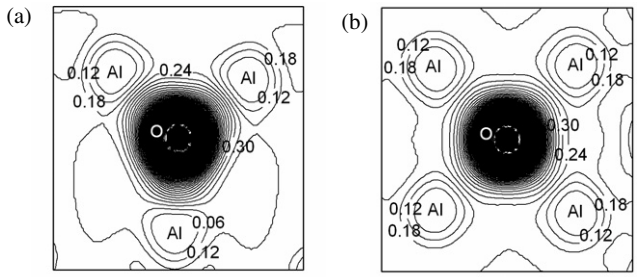

Figure 7. The charge distribution of the O atom with its first nearest-neighbor Al atoms (a) I10, (b) S5. The interval of the contours is 0.06 electrons Å^{-3}.

range of −10 to −7 eV for both I10 and S5 cases should also be related to the formation of the covalent-like O–Al bond containing the O 2p, Al 3s and 3p electrons.

The characteristic of the O–Al bond can also be partly reflected from the charge distribution plot; O bonds with three and four Al atoms in the I10 and S5 cases, respectively. Further, O and these Al atoms are almost coplanar in both cases. Figure 7 shows that the charge density is localized between the O atom and the surrounding Al atoms in these two cases, and the charge distributions show the directivity. This suggests that the O–Al bond contains covalent character and thus should be a stronger bond. This is consistent with our previous study for the NiAl bulk case [22].

3.5. Formation of a coplanar O–Al bonding cluster

It is very interesting to see that, for the low formation energy cases where O bonds with the Al atoms, O is approximately coplanar with its surrounding 1NN Al atoms. As shown in figure 3, for the I10 case, O bonds with three Al atoms (4, D_2, 2) in the (001) plane that is perpendicular to the GB plane, forming three coplanar equivalent O–Al bonds with bond lengths of 1.80 Å. After the substitution of O for the Ni atom 5, the O atom moves away from its original 1NN Ni atoms and goes into the NiAl GBs, forming an O–Al atomic coplanar cluster with one O atom and four Al atoms (4, 2, D_1, and B_1) with the equivalent four O–Al bond lengths of 1.97 Å. The Ni atom 1 locates in the center of the NiAl GB. Its replacement by O leads directly to the formation of an O–Al atomic coplanar cluster with one O atom and four surrounding Al atoms (4, D1, D2, D3) with the equivalent four O–Al bond lengths of 1.92 Å. The coplanar configurations of the S1 and S5 cases are almost the same and both are normal to the (001) plane. However, these two cluster planes form different angles with the GB plane. The formed cluster plane in the S1 case is indexed by $(1\bar{3}0)$ that is perpendicular to the GB plane. Further, the 2NNs of the O atom in these clusters are almost Ni atoms, with an average bond length of ∼3.0 Å, much larger than that of the 1NN O–Al bond. This is the reason why we can call these coplanar O and Al atoms 'clusters'.

The GB can be divided by two regions, the Al-rich region surrounded by Al atoms of 4, D_1, 2, B_1, D_2, D_3 and the Ni-rich region surrounded by Ni atoms of 3, C_1, 1, A_1, C_2, C_3. The O atom in all the above three cases (I10, S1, and S5) with lower formation energies locates in the Al-rich region. Such an Al-rich region is capable of 'drawing' the O atom in the GB to form an O–Al bonding coplanar cluster because O prefers to bond with Al rather than Ni, as illustrated above as well as in the study in the bulk [22]. This is why the O atom in the I10 and S5 case moves to the center of the GB after the relaxation.

However, it seems strange that, although O also forms a coplanar-like cluster with the surrounding four Al atoms (6, G, G_1, F_1, as shown in figure 3) in the S3 case, the O atom moves away from the GB, in contrast with the I10, S1, and S5 cases. The reason lies in the substitutional O atom for the Ni atom 3 being close to the Ni-rich region in the GB, thus going to the neighboring Al-rich region surrounded by the Al atoms of 6, G, G_1, and F_1. As shown in figure 3, in addition to the four Al atoms, O also bonds with one additional Ni atom (H) with a bond length of 2.11 Å because the O–Al cluster goes into the NiAl bulk. Such an additional Ni atom makes the O–Al cluster corrugated and the formation energy higher than the same substitutional S1 and S5 cases.

Since the O–Al bond is covalent-like and thus stronger, the formation of the coplanar O–Al bonding cluster in the NiAl GB will greatly affect the mechanical properties of NiAl. The NiAl GB can be embrittled due to such stronger O–Al cluster formation, and hence will not be beneficial to the plasticity of the NiAl intermetallics. We can predict that O aggregation in the NiAl GB can have a much larger effect on the mechanical properties of the NiAl. The results can also be referenced to the oxidation effect of O in the NiAl.

4. Conclusions

The site occupancy, energetics, structure, and bonding properties of O in a $\Sigma = 5$ NiAl grain boundary (GB) have been investigated by using a first-principles total energy method based on density functional theory with the generalized gradient approximation. O is shown to be preferable to segregate in the NiAl GB with a segregation energy of −1.75 eV, which implies that almost all the O will distribute in the GB instead of the bulk. The interstitial sites in the GB favor the O segregation as compared with the substitutional sites, according to the calculated formation energy results. The atomic configurations as well as the formation energy of O indicate that O likes to bond with Al instead of Ni in the NiAl GB due to the electronegativity difference between Al and Ni with reference to O, similar to the previous study for the NiAl bulk [22]. Charge distribution and the density of states further indicate the intrinsic bonding properties of O–Al, which contain covalent character and thus the O–Al bond should be stronger. Both the interstitial and substitutional cases exhibit different configurations from the bulk case due to the presence of GBs, in which O normally bonds with three to five Al or Ni atoms or both. Interestingly, a stronger coplanar O–Al bonding cluster forms in the NiAl GB for the lower formation energy cases, which can be considered to embrittle NiAl and thus will be deleterious to the plasticity of the NiAl intermetallics. Our results will provide a useful reference for understanding the effects of O on the mechanical properties as well as the oxidation effects of the NiAl intermetallics.

Acknowledgments

The research is supported by the Aeronautics Science Foundation of China (ASFC) with grant No. 2007ZF51071 and New Century Excellent Talents in University NCET-07-0040.

References

[1] Stoloff N S 1996 *Microstructure and Properties of Materials* vol 1, ed J C M Li (Singapore: World Scientific) pp 51–106
[2] Miracle D B and Darolia R 1995 *Intermetallic Compounds: Principles and Practice* vol 2, ed J H Westbrook and R L Fleischer (Chichester: Wiley) pp 53–72
[3] Song Y, Guo Z X, Yang R and Li D 2001 *Acta Mater.* **49** 1647
[4] Lazar P and Podloucky R 2006 *Phys. Rev.* B **73** 104114
[5] Noebe R D, Bowman R R and Nathal M V 1993 *Int. Mater. Rev.* **38** 193
[6] Briant C L and Messmer R P 1980 *Phil. Mag.* B **42** 569
[7] Liu C T and George E P 1997 *Int. Symp. on Nickel and Iron Aluminides: Processing, Properties, and Applications* ed S C Deevi *et al* (Materials Park, OH: ASM International) pp 21–31
[8] Lu G-H, Deng S, Wang T, Kohyama M and Yamamoto R 2004 *Phys. Rev.* B **69** 134106
[9] Lu G-H, Zhang Y, Deng S, Wang T, Kohyama M, Yamamoto R, Liu F, Horikawa K and Kanno M 2006 *Phys. Rev.* B **73** 224115
[10] Zhang Y, Lu G-H, Deng S, Wang T, Shu X, Kohyama M and Yamamoto R 2006 *J. Phys.: Condens. Matter* **18** 5121
[11] Zhang Y, Lu G-H, Deng S, Wang T, Xu H, Kohyama M and Yamamoto R 2007 *Phys. Rev.* B **75** 174101
[12] George E P and Liu C T 1990 *J. Mater. Res.* **5** 754
[13] Miracle D B 1993 *Acta Metall. Mater.* **41** 649
[14] Ren W, Guo J T, Li G and Zhuo J Y 2004 *J. Mater. Sci. Technol.* **20** 163
[15] Jayaram R and Miller M K 1995 *Scr. Metall. Mater.* **33** 19
[16] Kim T, Hong K T and Lee K S 2003 *Intermetallics* **11** 33
[17] Yan M, Vitek V and Chen S P 1996 *Acta Mater.* **44** 4351
[18] Xie X and Mishin Y 2002 *Acta Mater.* **50** 4303
[19] Brown J A and Mishin Y 2005 *Acta Mater.* **53** 2149
[20] Mutasa B and Farkas D 1998 *Metall. Mater. Trans.* A **29** 2655
[21] Raulot J M, Fraczkiewicz A and Cordonnier T 2008 *J. Mater. Sci.* **43** 3867
[22] Hu X L, Lu G-H, Zhang Y, Yin P G, Xiao P H, Wang T M and Xu H B 2008 *Intermetallics* at press
[23] Perdew J P and Wang Y 1992 *Phys. Rev.* B **45** 13244
[24] Kresse G and Hafner J 1993 *Phys. Rev.* B **47** 558
[25] Kresse G and Furthmüller J 1996 *Phys. Rev.* B **54** 11169
[26] Monkhorst H J and Pack J D 1976 *Phys. Rev.* B **13** 5188
[27] Fonda R and Luzzi D 1993 *Mater. Res. Soc. Symp. Proc.* **288** 361
[28] Fonda R W, Yan M and Luzzi D E 1995 *Phil. Mag. Lett.* **71** 221
[29] Djajaputra D and Cooper B R 2001 *Phys. Rev.* B **64** 085121
Djajaputra D and Cooper B R 2002 *Phys. Rev.* B **66** 205108
[30] Winter M 1993 *WebElements: the periodic table on the web* http://www.webelements.com